

A method for estimating time-dependent acoustic cross-sections of bubbles and bubble clouds prior to the steady state

J. W. L. Clarke and T. G. Leighton

Institute of Sound and Vibration Research, University of Southampton, Highfield, Southampton SO17 1BJ, United Kingdom

(Received 16 November 1998; revised 11 August 1999; accepted 21 September 1999)

Models for the acoustic cross-sections of gas bubbles undergoing steady-state pulsation in liquid have existed for some time. This article presents a theoretical scheme for estimating the cross-sections of single bubbles, and bubble clouds, from the start of insonation onward. In this period the presence of transients can significantly alter the cross-section from the steady-state value. The model combines numerical solutions of the Herring–Keller model with appropriate damping values to calculate the extinction cross-section of a bubble as a function of time in response to a continuous harmonic sound field (it is also shown how the model can be adapted to estimate the time-dependent scatter cross-section). The model is then extended to determine the extinction cross-section area of multiple bubbles of varying population distributions assuming no bubble–bubble interactions. The results have shown that the time taken to reach steady state is dependent on the closeness of the bubble to resonance, and on the driving pressure amplitude. In the response of the population as a whole, the time to reach steady state tends to decrease with increasing values of the driving pressure amplitude; and with the increasing values of the ratio of the numbers of bubbles having radii much larger than resonance to the number of resonant bubbles. The implications of these findings for the use of acoustic pulses are explored. [S0001-4966(00)01801-4]

PACS numbers: 43.25.Ts, 43.35.Ei, 43.30.Lz [DLB]

INTRODUCTION

It has long been recognized that the high impedance mismatch between an air-filled bubble and the surrounding water provides an excellent acoustic target owing to strong inert scattering. It is also well understood that enhanced scatter and dissipation result from the pulsations into which the bubble will be driven by the sound field. To a first order, this response can be modeled as that of a single degree of freedom system with a resonance frequency, which is dependent on bubble size, where the bubble response is a maximum. It has been convenient to define acoustic extinction and scatter cross-sections for single bubbles, given, respectively, by the ratio of the power lost or reradiated by the bubble to the intensity of an incident plane wave. These have been calculated for the steady state¹ showing that, for a given bubble size, they are maximal at the resonance frequency. It should be noted that the cross-sections are only local maxima at resonance if considered as a function of bubble size for a given insonification frequency. This is because the contribution due to inert scattering will steadily increase with bubble size.

The resonant and off-resonant scattering characteristics of bubbles are well defined and are utilized in a wide number of applications including measurement of oceanic bubble populations^{1–4} and research into upper ocean dynamics.⁵ However, it is these same characteristics which make acoustic detection of nonbubble targets in areas with high bubble populations (such as the surf-zone) difficult.

One possible solution to this problem utilizes the bubble ‘ring-up’ time, based on the time taken for a bubble to reach steady-state oscillation. Theory suggests that, owing to inertial effects, this ring-up time will be finite and that prior to reaching steady-state oscillation the acoustic scattering

will be greatly reduced. A reduction in scattering attributed to ‘ring-up’ time effects was first detected by Akulichev⁶ in 1985. However two more recent studies^{7,8} have failed to measure any reduction in scattering.

This letter outlines a theoretical scheme which enables the investigation of ring-up times of gas bubbles in fresh water. The model has also been used to determine the extinction cross-section area of bubble clouds of varying population distributions in a 150-kHz sound field assuming no bubble–bubble interactions. This model has been used to help ascertain a possible reason why Suiter⁷ and Pace *et al.*⁸ did not detect any reduction in scattering.

I. THEORETICAL MODELING OF THE RESPONSE OF A BUBBLE

As discussed in the Introduction, a gas bubble in water, when insonified by a plane wave, will pulsate. The oscillation is, at least to a first approximation, that of a single degree of freedom system, assuming small amplitude oscillations. In this case the restoring force is the elasticity of the gas and the mass is the effective inertia of the liquid component of the oscillating bubble. Damping, and thus energy loss, is introduced into the system by three distinct mechanisms:⁹ energy radiated away from the bubble as acoustic waves (radiation damping); energy lost through thermal conduction between the gas and the surrounding liquid (thermal damping); and work done against viscous forces at the bubble wall (viscous damping).

Therefore a simple equation of motion, in the radius-force frame, for such a system driven at a single frequency would be

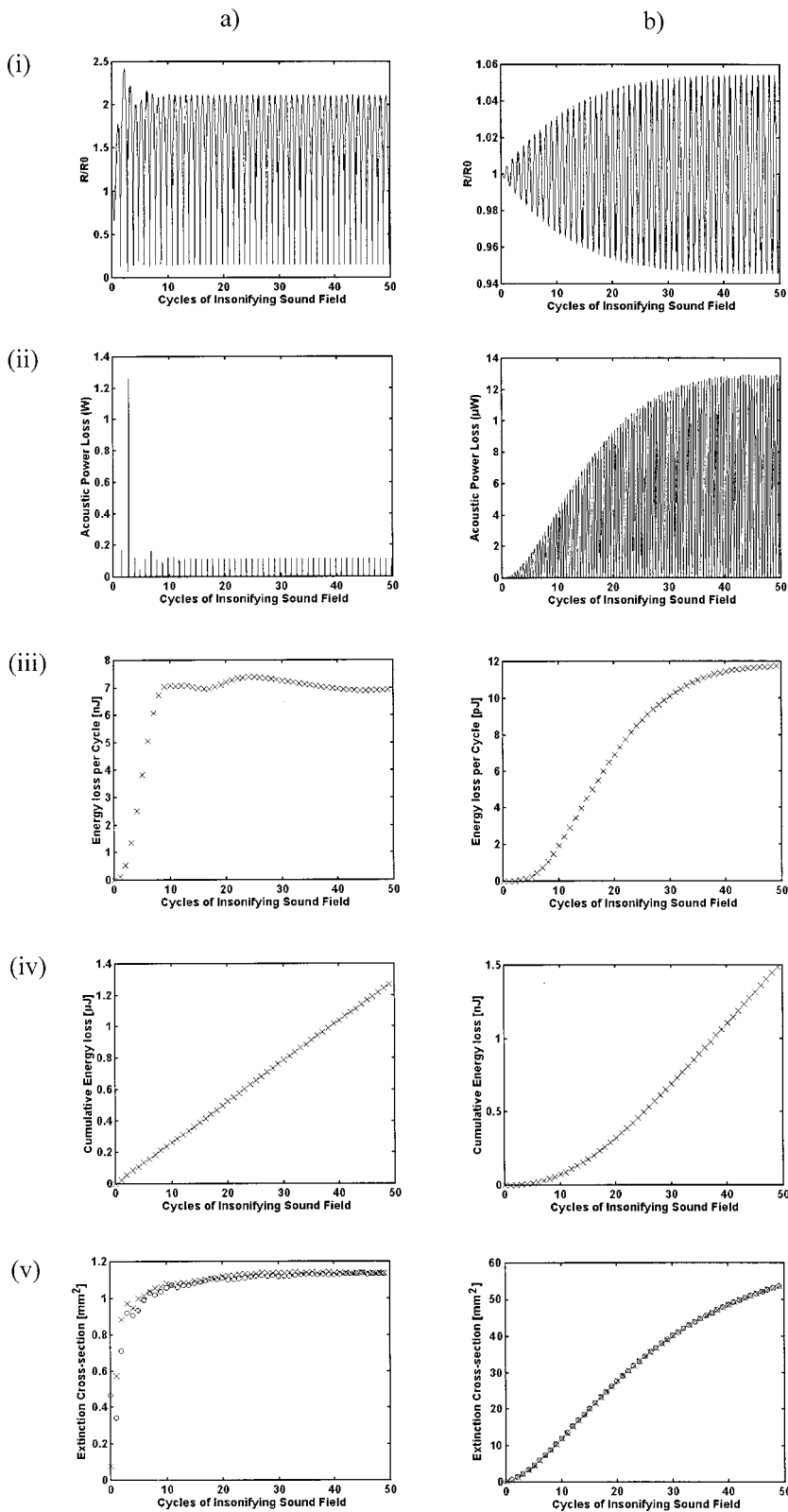


FIG. 1. Simulations of a 20- μm radius bubble in a 150-kHz (a) 1×10^5 Pa, (b) 500 Pa sound field. (i) Bubble wall displacement; (ii) the instantaneous power loss; (iii) energy loss over each cycle of the insonifying sound field; (iv) cumulative total energy loss; (v) extinction cross-sectional area of the bubble over each cycle of the insonifying sound field. For comparison the extinction cross-section calculated using the Gilmore model is also plotted in part (v) (“ \circ ” Gilmore, “ \times ” Keller–Miksis). The steady-state extinction cross-sectional area for a 20- μm bubble driven at resonance according to linear theory (Ref. 16) is 6.68×10^{-5} m^2 .

$$m_{\text{rad}}^{\text{RF}} \ddot{R} + b_{\text{tot}}^{\text{RF}} \dot{R} + kR = -P_A \times 4\pi R_0^2 \cos(\omega t), \quad (1)$$

where $m_{\text{rad}}^{\text{RF}}$ is the inertia of the system, $b_{\text{tot}}^{\text{RF}}$ is the total damping in the radius-force frame, k is the stiffness, R is the radius of the bubble, R_0 is the equilibrium radius, P_A the acoustic pressure amplitude, and ω is the angular frequency of the driving sound field.¹⁰ This is appropriate for bubble pulsations of small amplitude.

The rate of loss of energy (power loss) subtracted from the incident wave by the bubble is:

$$\text{Power} = b_{\text{tot}}^{\text{RF}} \dot{R}^2. \quad (2)$$

Twice during each bubble oscillation, $\dot{R} = 0$. Consider two consecutive times, t_n and t_{n+1} when this occurs. The energy lost from an incident plane wave through viscous, thermal

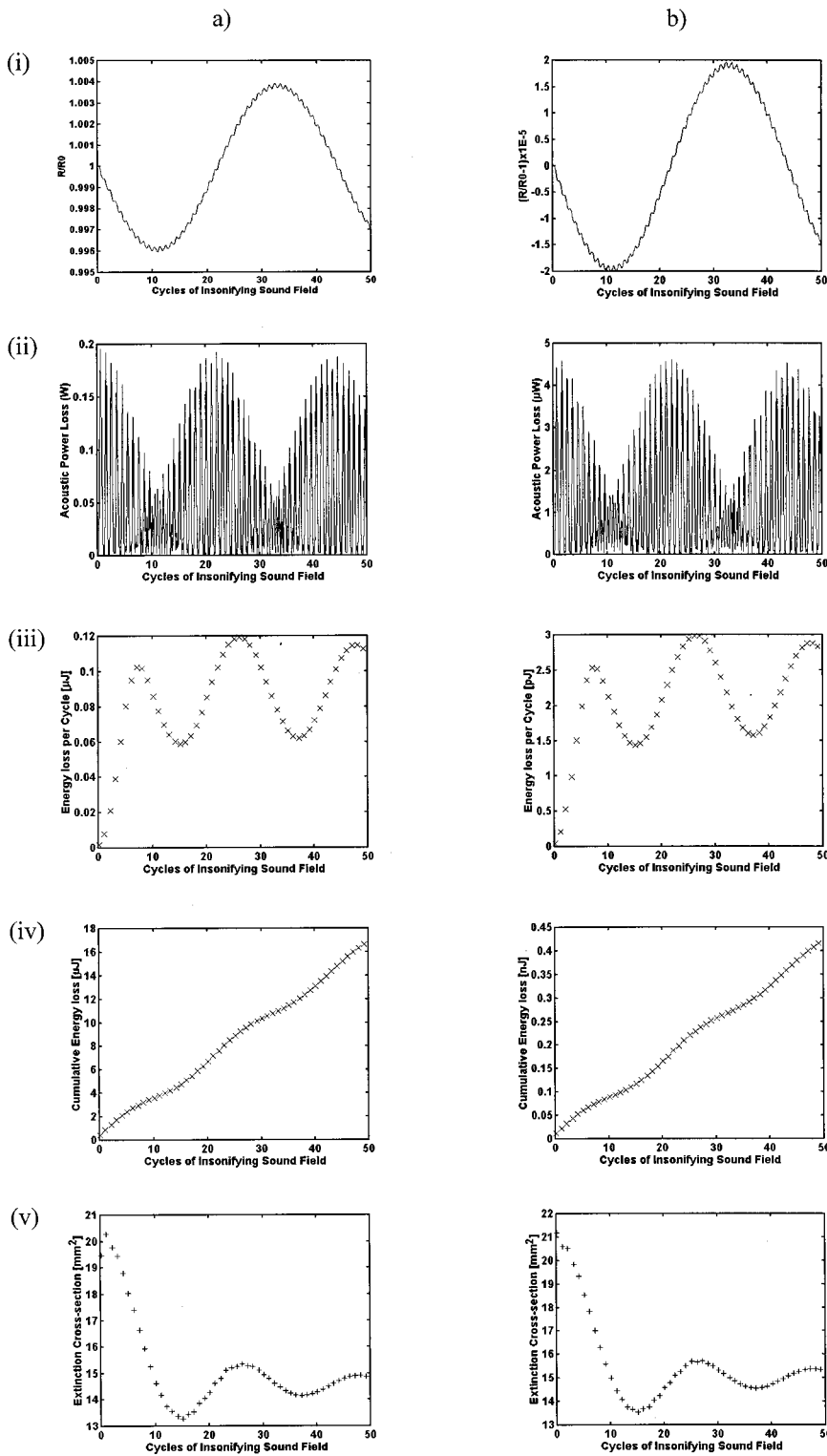


FIG. 2. Simulations of a 1-mm radius bubble in a 150-kHz (a) 1×10^5 Pa, (b) 500 Pa sound field. (i) Bubble wall displacement [for (b) the y-axis has been changed to show $(R/R_0 - 1)$ so that the axis values can be more clearly shown]; (ii) the instantaneous power loss; (iii) energy loss over each cycle of the insonifying sound field; (iv) cumulative total energy loss; (v) extinction cross-sectional area of the bubble over each cycle of the insonifying sound field. The steady-state extinction cross-sectional area for a 1-mm bubble driven at resonance according to linear theory (Ref. 16) is 1.03×10^{-5} m².

and scattering losses in the interval $t = t_n$ to $t = t_{n+1}$ is:

$$\Phi_n = \int_{t=t_n}^{t=t_{n+1}} b_{\text{tot}}^{\text{RF}} \dot{R}^2 dt, \quad (3)$$

and the average power loss in this interval is:

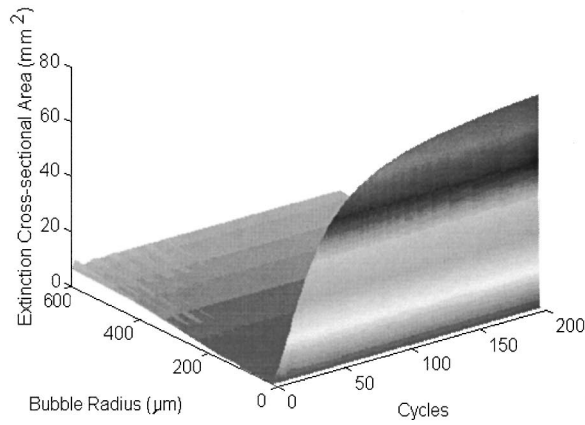
$$\langle W_n \rangle = \frac{\Phi_n}{t_{n+1} - t_n}. \quad (4)$$

It is then a simple matter to calculate the extinction cross-sectional area, Ω_n , appropriate to the time interval $t = t_n$ to

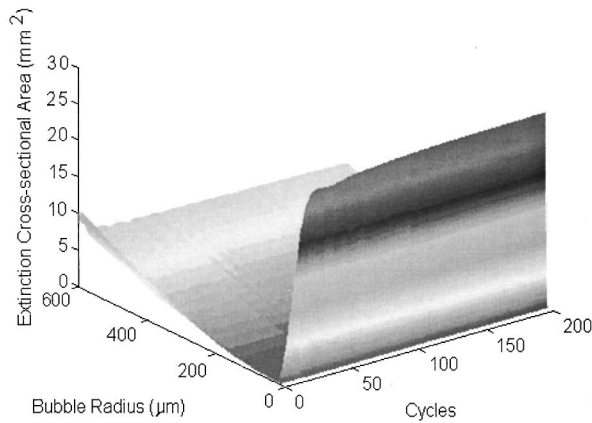
$t = t_{n+1}$. This is given simply by the ratio of the average power loss in this period to the intensity of the incident plane wave:

$$\Omega_n = \frac{\langle W_n \rangle}{I} = \frac{\int_{t=t_n}^{t=t_{n+1}} b_{\text{tot}}^{\text{RF}} \dot{R}^2 dt}{I(t_{n+1} - t_n)}. \quad (5)$$

It should be noted that if, instead of the total energy loss from the incident beam, it was the power scattered by the



a)



b)

FIG. 3. Extinction cross-sectional area of a single bubble of radius up to 600 μm in a 150-kHz sound field of amplitude (a) 500 Pa, (b) 5000 Pa. For clarity in plotting, the discrete function Ω_n shown in part (v) of Figs. 1 and 2 has been interpolated to provide line plots for the cross-sections shown in this figure and subsequent ones.

bubble which was of interest, then the above formulation can be simply adapted by employing only that component of the damping term $b_{\text{tot}}^{\text{RF}}$ which relates to radiated losses ($b_{\text{rad}}^{\text{RF}}$). This would give the acoustic scattering cross-section. However, a more exact form can be obtained by rewriting the scattered power in Eq. (5) in terms of the emitted pressure field, which can be formulated¹⁰ in terms of the bubble wall motion:

$$\Omega_n = \frac{\langle W_n \rangle}{I} = \frac{4\pi r^2 \int_{t=t_n}^{t=t_{n+1}} \frac{\left(\frac{\rho R}{r}(\ddot{R}R + 2\dot{R}^2)\right)^2}{\rho_0 c} dt}{I(t_{n+1} - t_n)}, \quad (6)$$

where r is the distance from the bubble, ρ_0 is the fluid density, and c is the speed of sound.

Bubbles are nonlinear oscillators and as the following analysis shows the ring-up time is dependent on the bubble equilibrium radius, the driving frequency, and the sound pressure level.

II. TIME-DEPENDENT EXTINCTION CROSS-SECTION OF A SINGLE BUBBLE

To calculate the time-dependent extinction cross-sectional area from Eq. (5), it is necessary to calculate the velocity of the bubble wall over time as well as the total damping in the radius-pressure frame. Although several options are available,¹¹ in this paper \dot{R} was found using the nonlinear bubble wall velocity determined from the Keller and Miksis equation¹² a form of the equations of motion first introduced by Herring.¹³

The damping term $b_{\text{tot}}^{\text{RF}}$ is obtained using Prosperetti's 1977 analysis.¹⁴ This is a linearized theory for the small amplitude forced pulsation of a bubble, describing the thermal effects in terms of the effective polytropic index and thermal damping constant. This analysis assumes a linear regime. Therefore the only expression of the bubble nonlinearity in this system comes from the Keller–Miksis equation (or equivalent). The resultant is therefore an approximation only. Thus care should be taken when considering the absolute values of $b_{\text{tot}}^{\text{RF}}\dot{R}^2$, especially for higher sound pressure levels when bubble motion is highly nonlinear, as a significant error in the calculation is likely. As discussed in Sec. I, computation of the scattering cross-section need not be limited by such linearizations, since small amplitude expressions for viscous and thermal losses are not required.

Figures 1 and 2 show four illustrative cases, and each figure is subdivided into five subsections [(i)–(v)] showing, against a common time axis, the following: (i) the normalized bubble radius; (ii) the instantaneous power loss determined from Eq. (2); (iii) the energy loss per cycle of the insonifying sound field as determined from Eq. (3) (plotted discretely for each cycle); (iv) a cumulative plot of the energy loss; (v) the time-dependent extinction cross-section area for a single bubble, Ω_n , as calculated by Eq. (5). Plot (iv) is particularly interesting. Were a bubble to immediately attain steady state, this plot would be a straight line of constant positive gradient. However, if the energy loss is less in the ring-up period, the plot will dip below the straight line which would be drawn if the eventual steady-state behavior were extrapolated to time zero.

Figure 1 shows the time-dependent extinction cross-sectional area of a resonant bubble in a 150 kHz sound field of amplitude 10^5 Pa [Fig. 1(a)] and 500 Pa [Fig. 1(b)]. Figure 2 shows the response of a 1-mm radius, off-resonant, bubble in the same sound fields. Further discussion of these results is included in Sec. IV below.

III. TIME-DEPENDENT EXTINCTION CROSS-SECTIONAL AREA OF A BUBBLE CLOUD

The above analysis can be expanded to give a first-order estimation of the time-dependent extinction cross-section of a bubble cloud. It is assumed that the number density is sufficiently small that bubble–bubble interactions can be neglected, as is the reduction in intensity of the incident wave as it propagates through the cloud (although a second-order calculation could include this). This article is restricted to a first-order calculation and thus will underestimate the extinction cross-section near to resonance.¹⁵ After calculating the

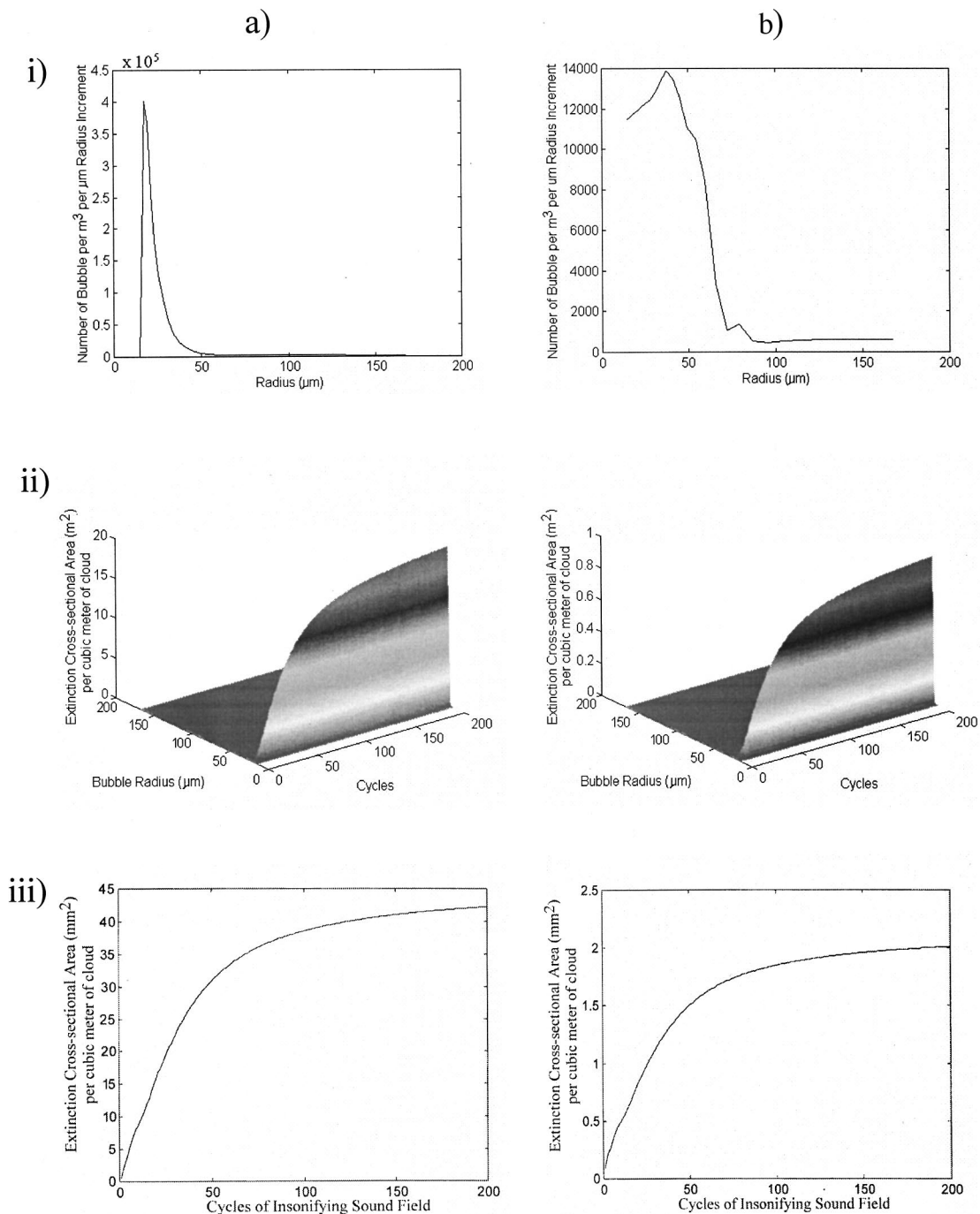


FIG. 4. Response of (a) an example oceanic bubble population (based on the measurements of Phelps and Leighton, Ref. 15); and (b) a laboratory bubble population (based on the measurements of Pace *et al.*, Ref. 8) in a 500-Pa, 150-kHz sound field. Plot (i) shows the bubble population distribution, (ii) is the extinction cross-sectional area of a 1 m^3 cloud, resolved for each radius bubble assuming no interactions, and (iii) is the extinction cross-sectional area of the 1 m^3 cloud (i.e., summed for all radii for each cycle of the sound field).

extinction cross-sectional area of a single bubble of varying radii and compiling the results as in Fig. 3, the effective response of a bubble layer with a given population distribution can be calculated. The density of the population is used as a scaling quantity given the limitations discussed above.

Therefore the response of a nonuniform bubble distribution can be investigated by multiplying the response [calculated as for Fig. 1(a) and (b)] by a population distribution. In addition the total response of the bubble cloud can be ascertained by integrating to find the area under the extinction cross-section radius curve for each cycle of the insonifying

sound field. Figures 4 and 5 show the response for a bubble population typical of an oceanic bubble cloud¹⁶ and an artificially produced bubble cloud (taken from the population measurements of Pace *et al.*⁸) in sound fields of 500 Pa and 5000 Pa amplitude. Since the acoustic attenuation method used for measuring the laboratory population proved unreliable for larger bubble sizes in the data of Pace *et al.*,⁸ their population has been extrapolated in Fig. 6, up to a radius of 600 μm , to investigate the effect that this could have on the time dependent extinction cross-sectional area (this is for illustrative purposes only and in no way suggests that this

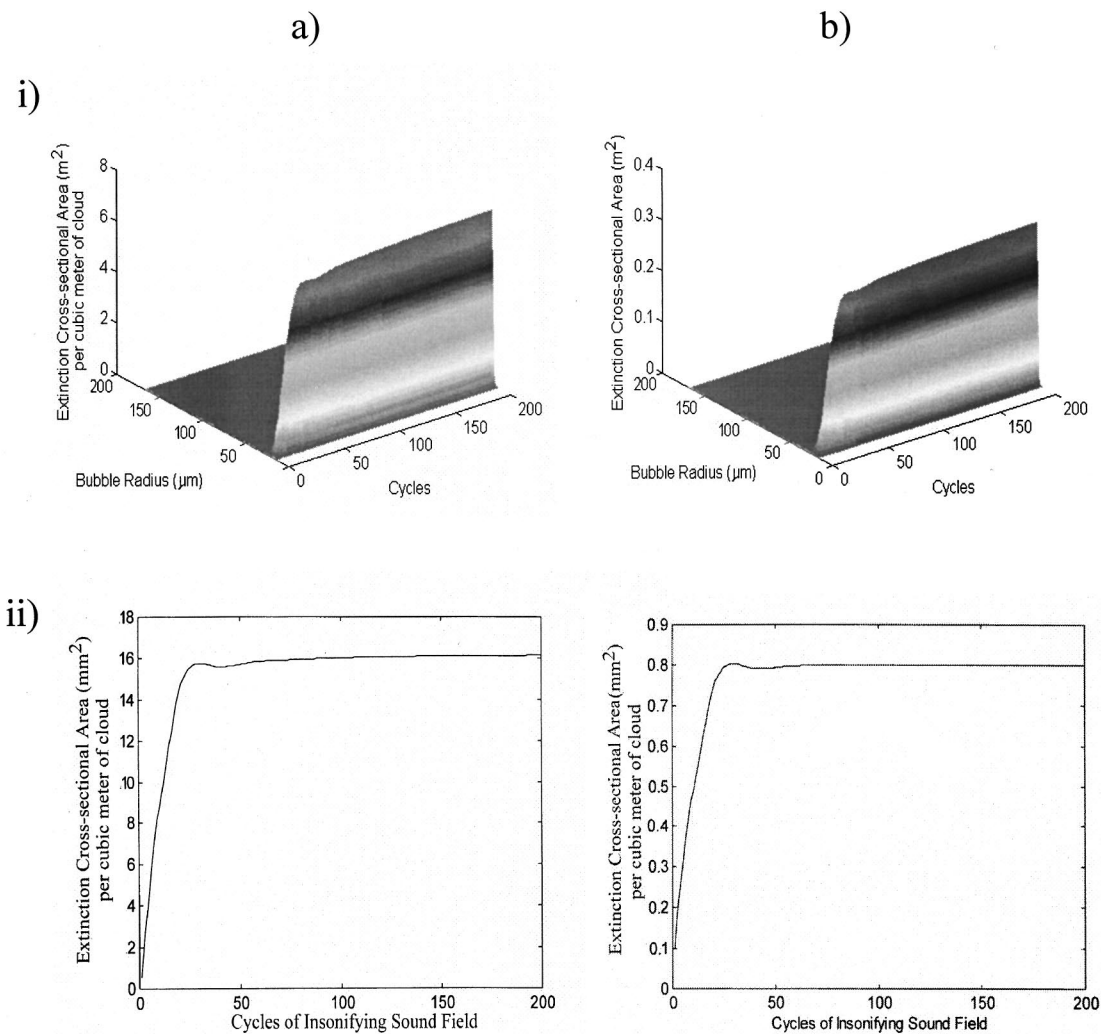


FIG. 5. Response of (a) an example oceanic bubble population (based on the measurements of Phelps and Leighton, Ref. 15) and (b) a laboratory bubble population (based on the measurements of Pace *et al.*, Ref. 8) in a 5000-Pa, 150-kHz sound field. (i) The extinction cross-sectional area of a 1 m³ cloud, resolved for each radius bubble assuming no interactions. (ii) The extinction cross-sectional area of the 1 m³ cloud (i.e., summed for all radii for each cycle of the sound field).

extrapolation reflects the true nature of the population).

IV. DISCUSSION

A simple comparison of the bubble wall displacements depicted in Figs. 1 and 2 provides an intuitive guide as to the effect of sound pressure level and the closeness to resonance on ring-up time. It can clearly be seen that the time taken to reach steady state is by far the longest for a resonant bubble in a low amplitude sound field. A gentle build-up to steady state is observed [Fig. 1(b)]. Conversely a resonant bubble in a high amplitude sound field exhibits a distinctly nonlinear response with significant initial transient activity before quickly achieving a steady-state response [Fig. 1(a)]. Examination of the off-resonant bubble wall displacement plots shows a reduced dependence on sound pressure level and a rapid rise time with subsequent reduction and oscillation (Fig. 2).

In the case of the resonant bubbles, the graphs of the extinction cross-sectional area shown in Fig. 1 tend to follow the mean bubble wall response exhibiting a brief, transient, ring-up at high sound pressure levels and a gradual build-up

for low sound pressure levels. The latter indicates potential for reducing losses by using short pulses of ultrasound, an effect confirmed by noting that in Fig. 1(b) (iv), in the first 30 cycles the curve dips below a straight line which might be extrapolated back from the steady state (as predicted in Sec. II).

A superposition of natural and driving frequencies is evident in the radius plots [Fig. 2(i)]. The extinction cross-sectional area for these off-resonant bubbles [Fig. 2(v)] is more complicated and can be more easily understood by examining the plots of the acoustic power loss determined from Eq. (2) [Fig. 2(ii)].

Although transients are more evident at the lower driving pressures [Fig. 2(b) (ii)], the tendency in both plots is for the energy loss [Fig. 2(iii)] and extinction cross-section [Fig. 2(v)] to oscillate around the steady-state value at twice the bubble natural frequency, although the cross-section takes much higher values for the first few cycles. Clearly the presence of such bubbles would not be conducive to enhancing acoustic transmission using pulsed fields. Figure 3 summarizes the time-dependent cross-section of single bubbles. A

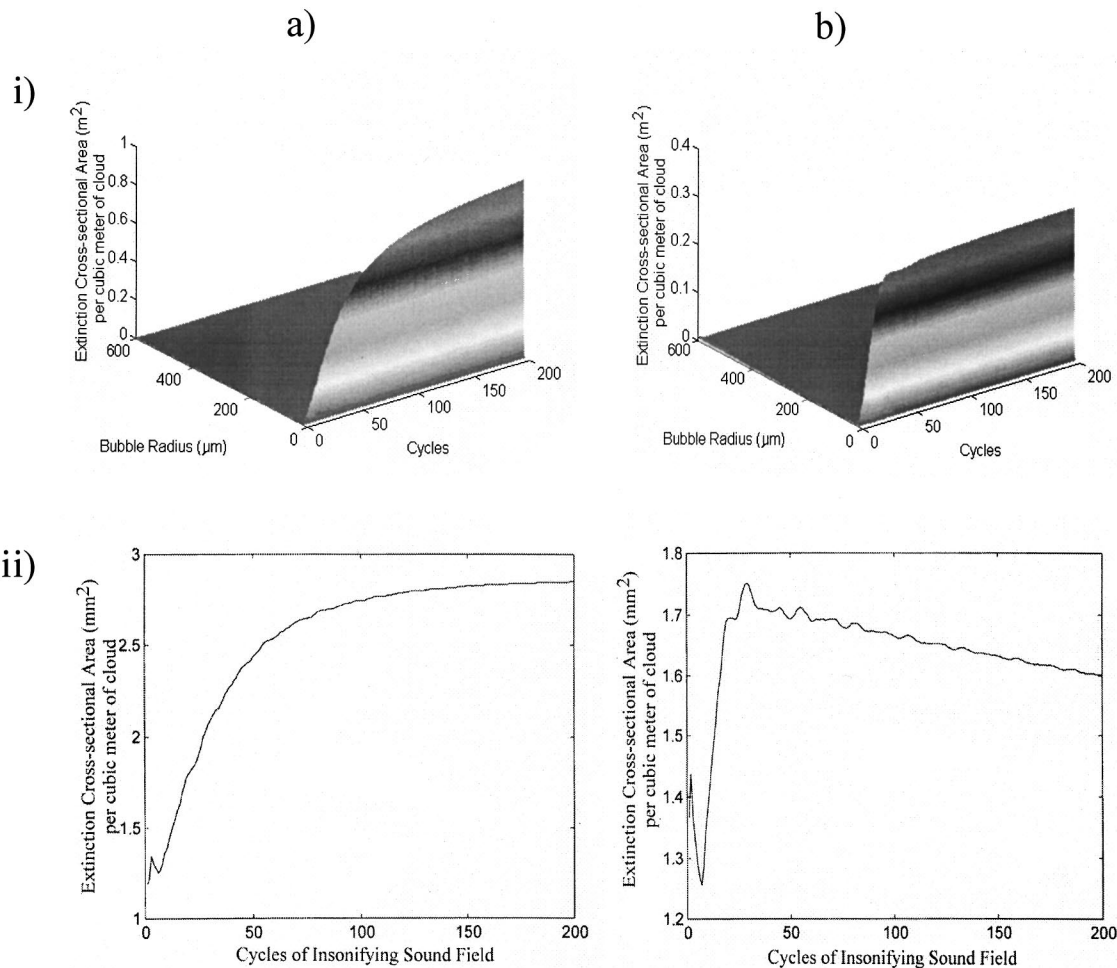


FIG. 6. Response of the laboratory bubble population (based on the measurements of Pace *et al.*, Ref. 8) extrapolated to include potential large bubbles in a 150-kHz, (a) 500 Pa and (b) 5000 Pa sound field. Plot (i) is the extinction cross-sectional area of a 1 m^3 cloud, resolved for each radius bubble assuming no interactions, and (ii) is the extinction cross-sectional area of a 1 m^3 cloud, summed for all radii for each cycle of the sound field.

“geometrical” contribution is seen from the large bubbles, which oscillate for a few tens of cycles following the onset of insonation around the eventual steady-state value. Smaller bubbles contribute a lesser amount except around the resonance condition. Here there is a peak, with a ring-up time

which tends to decrease with increasing driving amplitude. Figure 7 shows how the extinction cross-section of a $20\text{-}\mu\text{m}$ radius bubble changes with increasing sound pressure levels. The bubble response quickly deviates from an exponential ring-up with a corresponding decrease in ring-up time. Thus for the simulated response of a bubble cloud, which contain large numbers of small bubbles, to a 150-kHz sound field the response of the resonant bubble is dominant with a well defined ring-up time for low sound pressure levels (Fig. 4). It is evident that an increase in the sound pressure level can significantly reduce the ring-up time. The results shown in Fig. 5 demonstrate this effect. In the case of the extrapolated bubble populations shown in Fig. 6, despite the numbers of large bubbles being relatively few, their presence has a significant effect on the response of the cloud as a whole, particularly during the first few cycles of the insonifying sound field. In this epoch, the early motion of these large bubbles (characterized above as being a fall in the first few cycles following oscillation toward steady state) appears to dominate. Thus the presence of large bubbles and/or high sound pressure levels can be counter-indicative for the enhanced efficiency of penetration of sonar through bubble clouds.

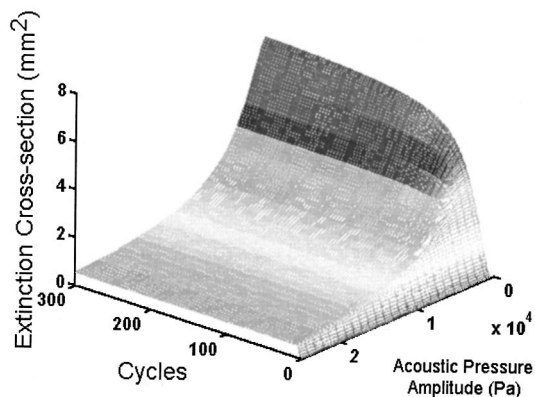


FIG. 7. Extinction cross-sectional area of a single bubble of radius $20 \mu\text{m}$ in a 150-kHz sound field of varying sound pressure level between 500 and 25 000 Pa.

V. CONCLUSIONS

A theoretical study into the time dependence of the response of air bubbles in fresh water to a continuous wave of 150-kHz sound field has shown that the ring-up time of a bubble is affected by its closeness to resonant oscillation and the amplitude of the driving sound field. Expansion of this theory to investigate the response of a low density bubble cloud of oceanic and laboratory origins has shown that a significant ring-up time should be detectable if the predominant smaller bubbles are insonified at their resonant frequency. Furthermore, higher sound pressure levels can obscure the ring-up time of the resonant bubbles, and the presence of large off-resonant bubbles even in relatively small quantities can enhance this effect significantly.

ACKNOWLEDGMENTS

The authors wish to acknowledge funding from the Defence Evaluation Research Agency (Contract No. SSDW1/647) and are very grateful to G. J. Heald and H. A. Dumbrell of DERA Bingley for invaluable scientific and technical input.

¹H. Medwin, "Counting bubbles acoustically: A review," *Ultrasonics* **15**, 7–14 (1977).

²D. M. Farmer and S. Vagle, "Bubble measurements using a resonator system," in *Natural Physical Processes Associated with Sea Surface Sound*, edited by T. G. Leighton (University of Southampton, 1997), pp. 155–162.

³W. K. Melville, E. Terrill, and F. Veron, "Bubbles and turbulence under breaking waves," *Natural Physical Processes Associated with Sea Surface Sound*, University of Southampton, edited by T. G. Leighton (1997), pp. 135–145.

⁴A. D. Phelps, D. G. Ramble, and T. G. Leighton, "The use of a combination frequency technique to measure the surf zone bubble population," *J. Acoust. Soc. Am.* **101**, 1981–1989 (1997).

⁵S. A. Thorpe, "Bubble clouds and the dynamics of the upper ocean," *Q. J. R. Meteorol. Soc.* **118**, 1–22 (1992).

⁶V. A. Akulichev, V. A. Bulanov, and S. A. Klenin, "Acoustic sensing of gas bubbles in the ocean medium," *Sov. Phys. Acoust.* **32**, 177–180 (1986).

⁷H. R. Suiter, "Pulse length effects on the transmissivity of bubbly water," *J. Acoust. Soc. Am.* **91**, 1383–1387 (1992).

⁸N. G. Pace, A. Cowley, and A. M. Campbell, "Short pulse acoustic excitation of microbubbles," *J. Acoust. Soc. Am.* **102**, 1474–1479 (1997).

⁹C. Devin, Jr., "Survey of thermal, radiation, and viscous damping of pulsating air bubbles in water," *J. Acoust. Soc. Am.* **31**, 1654 (1959).

¹⁰T. G. Leighton, *The Acoustic Bubble* (Academic, New York, 1994), Sections 3.3.1(b), 3.2.1, and 4.1.2.

¹¹For comparison the Gilmore equation was also used to determine \dot{R} with, as Fig. 1(v) illustrates, negligible effect for the parameter range indicated here.

¹²J. B. Keller and M. Miksis, "Bubble oscillations of large amplitude," *J. Acoust. Soc. Am.* **68**, 628–633 (1980).

¹³C. Herring, "Theory of the pulsations of the gas bubble produced by an underwater explosion," OSRD, Rep. No. 236 (1941).

¹⁴A. Prosperetti, "Thermal effects and damping mechanisms in the forced radial oscillations of gas bubbles in liquids," *J. Acoust. Soc. Am.* **61**, 17–27 (1977).

¹⁵Z. Ye and L. Ding, "Acoustic dispersion and attenuation relations in bubbly mixture," *J. Acoust. Soc. Am.* **98**, 1629–1636 (1995).

¹⁶A. D. Phelps and T. G. Leighton, "Oceanic bubble population measurements using a buoy deployed combination frequency technique," *IEEE J. Ocean Eng.* **23**, 400–410 (1998).